Sensor and Simulation Notes

Note 464

January 2002

Fabrication and Testing of a Membrane IRA

Leland H. Bowen and Everett G. Farr
Farr Research, Inc.

James P. Paxton and Andrew J. Witzig
Physitron, Inc.

Carl E. Baum, Dean I. Lawry, and William D. Prather
Air Force Research Laboratory, Directed Energy Directorate

Abstract

We describe here the development and testing of the prototype Membrane IRA, along with a set of preliminary experiments. In the first experiment, we developed a new feedline and balun configuration that can provide a well matched, relatively low loss feed for the antenna. In the second experiment, we determined a reliable etching process to remove the metallization from the membrane. This was required to shape the aperture and feed arms. Finally, using both calculations and measurements, we showed that the conductor thickness (300 Å aluminum) was sufficient to provide adequate conductivity for good reflection from the metallized membrane reflector. Based on these experiments, a prototype membrane IRA was designed and tested.

This work was funded in part by the Air Force Office of Scientific Research, Alexandria, VA, and in part by the Air Force Research Laboratory, Directed Energy Directorate, under contract F29601-01-C-0100.

I. Introduction

Compact Ultra-Wideband (UWB) antennas could be of great use in a variety of space-based applications, including radar, communications, and surveillance. The challenge is to deploy a lightweight UWB antenna that is stowable in a small volume, that is automatically deployable, and that will be resistant to the harsh space environment.

As a first step in overcoming these challenges, we designed, constructed and tested a prototype inflatable impulse radiating antenna fabricated from a thin membrane of aluminized Kapton®. The new design is called a Membrane Impulse Radiating Antenna, or Membrane IRA. The Membrane IRA is a blend of two well-established foundation technologies. The first of these is the Collapsible Impulse Radiating Antenna (CIRA), which has an umbrella-like design[1]. The second foundation technology is inflatable large-aperture reflectors fabricated from membranes such as Kapton® or Mylar®.

The currently available CIRA design is too large (when collapsed) and heavy for space applications. Our design for the Membrane IRA was based on that of the CIRA, which is 1.22 m (48″) in diameter and has 12 panels in the reflector. However, there are two major differences between the CIRA and the Membrane IRA. First, the Membrane IRA is constructed from a Kapton® film, which is very thin and lightweight. Second, the Membrane IRA is deployed and mechanically supported by inflation with low-pressure gas, rather than having an umbrella like frame as is the case with the CIRA.

We describe here the development and testing of the Phase I Membrane IRA, along with a set of preliminary experiments. These experiments include tests on a new feedline and balun configuration, tests on the etching process used to shape the aperture, and calculations and measurements of the conductor thickness required.

We begin now with experiments on the balun and feed network.

II. Balun/Twinline Experiments.

First, we describe our experiments with the new balun and feedline configuration. This new configuration was needed because the coaxial cables that are normally used in our CIRA designs have a large bend radius and cannot be stored compactly. For that reason, we experimented with building a 200-ohm differential-mode transmission line that is fed up the axis of the reflector. To feed this line, we built a new splitter balun consisting of two 100-ohm cables connected in parallel at the 50-ohm cable input and in series at the connection to the 200-ohm feedline. Ferrite beads are placed on the 100-ohm cables for isolation.

Our early feedline experiments used two round wires, but our prototype antenna used two narrow strips of copper tape. Both configurations are shown in Figure 2.1. In the future, we expect to print or plate conductive strips onto a Kapton® membrane. The impedance of the twinline with round conductors is given by [2]

$$Z_0 = \frac{377}{\pi\sqrt{\varepsilon_r}} \cosh^{-1}(D/d) = 200\Omega \qquad (1)$$

where D and d are defined in Figure 2.1. For our experiments we used 20-gauge wire (d = 0.81mm (0.032″)), so the spacing between the wires was D = 2.2 mm (0.087″).

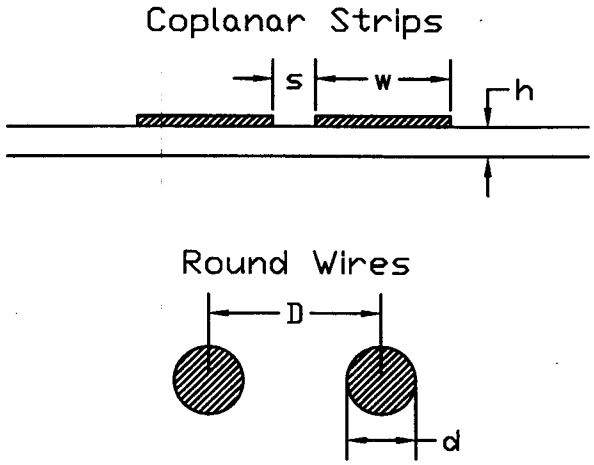

Figure 2.1. Plated twinline (top) and round wires (bottom).

To test the transmission-line/balun combination, we launched a signal onto the line, reflecting it off an aluminum sheet at the far end, and we measured the returned signal. A photo of the overall experiment is shown in Figure 2.2 on the left, and a detail of the balun is shown on the right. The balun is approximately 114 mm (4.5″) across. The size and weight of the balun can be further reduced for actual use in space.

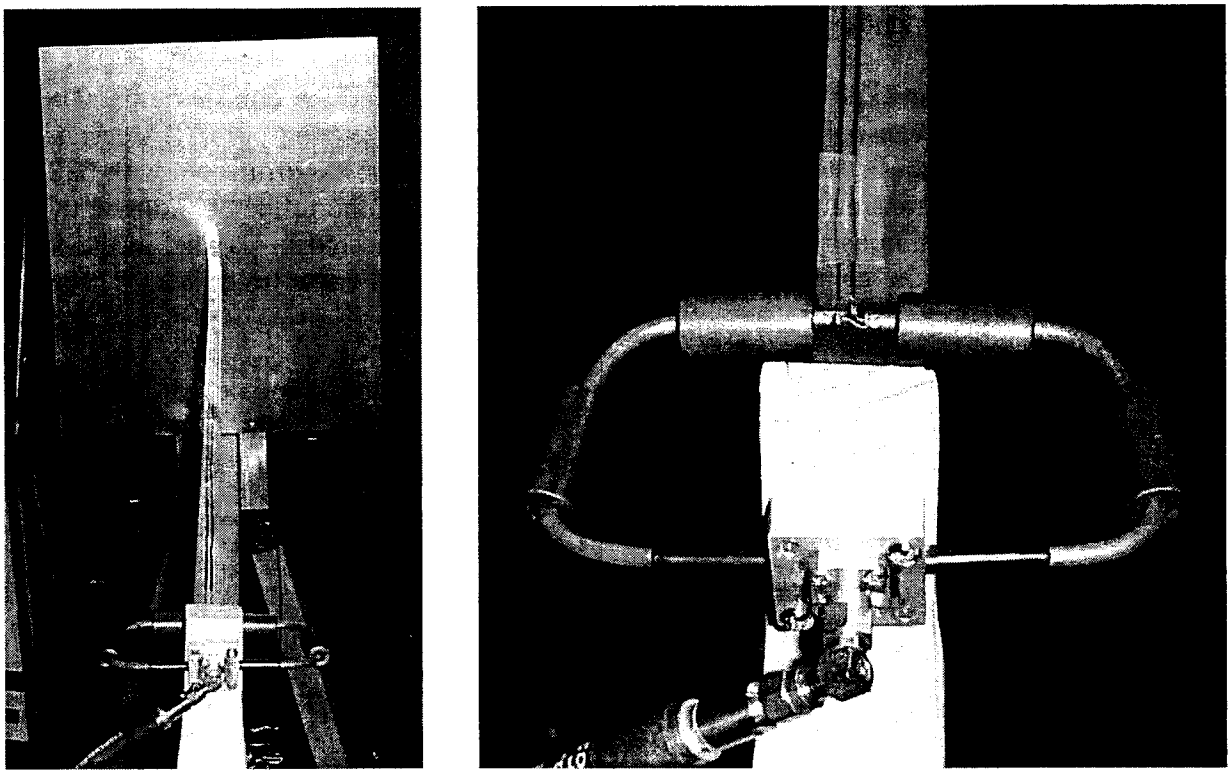

Figure 2.2. Experimental setup for the twinline experiment.

To determine the attenuation of the line, TDRs were taken with the twinline shorted at the near and far ends. The twinline was 1 meter long. The derivative of each TDR was then clipped to remove unnecessary information. The ratio of the two TDRs represents the impulse response, $h(t)$, of the round-trip propagation over the transmission line. We assume that a model for this propagation function or impulse response is of the form

$$h(\omega) = \frac{d/dt\left(\text{TDR}_{\text{shorted at far end}}\right)}{d/dt\left(\text{TDR}_{\text{shorted at near end}}\right)} = e^{2L\alpha(\omega)}\, e^{j2L\omega/c} = e^{2L(\alpha(\omega)+j\omega/c)} \qquad (2)$$

where $2L$ is the two-way length of the transmission line. We assume that the loss function, $a(\omega)$, is a real-valued function of frequency. We now adjust the time delay of $h(t)$ so that the peak occurs at $t= 0$. This has the effect of unwrapping the phase in the frequency domain. So the time-shifted version of the impulse response of the transmission line is just

$$h_{shifted}(\omega) = e^{2L\alpha(\omega)} \qquad (3)$$

At this point, we checked $h_{shifted}(\omega)$ to verify that the phase is approximately equal to zero up to some high frequency (> 5 GHz or so). We found that indeed to be the case. The attenuation in decibels as a function of frequency is now just

$$\text{atten}\big|_{dB} = -20\log_{10}\left|h_{shifted}(\omega)\right| \qquad (4)$$

Finally, the attenuation in decibels per meter is

$$\text{atten}\big|_{dB/m} = -\frac{20}{2L}\log_{10}\left|h_{shifted}(\omega)\right| \tag{5}$$

In Figure 2.3, we have plotted the attenuation for a 487 mm (19.2″) length of line, which would be found in a 1.22 m (48″) diameter IRA with $F/D = 0.4$. For this case, the attenuation is less than 2 dB up to around 8 GHz. This attenuation will be acceptable for the range of frequencies we are likely to need.

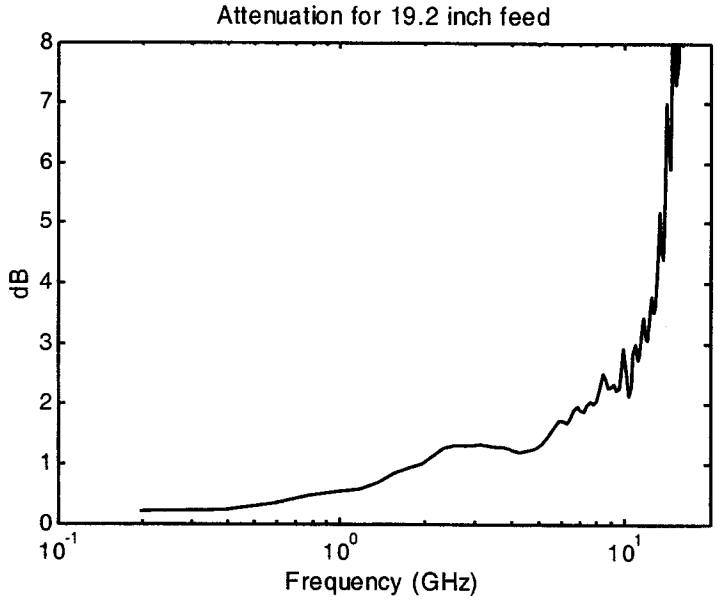

Figure 2.3. Attenuation for a twinline that is 0.487 m (19.2″) long.

Next we measured the attenuation of the balun alone, by taking the TDR of the balun with the output shorted. This resulted in the Moebius Gap configuration shown in Figure 2.4. We then took the TDR with a short in place of the balun. Using these two TDRs, we computed the attenuation for a one-way transit through the balun, using the same technique described above for the twinline. The attenuation as a function of frequency is shown in Figure 2.5.

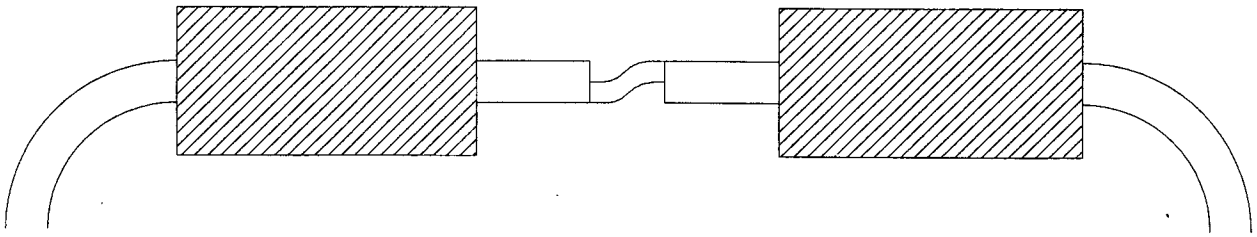

Figure 2.4. Moebius Gap including ferrite beads on 100 Ω coax cable.

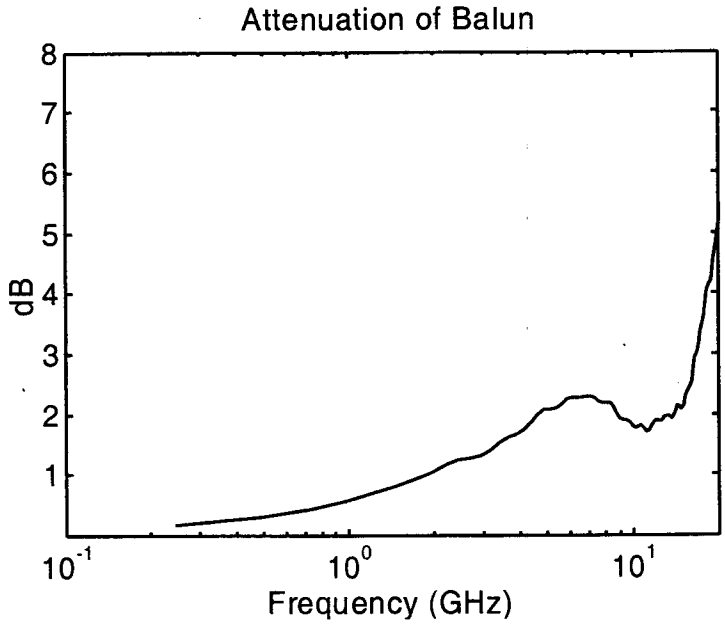

Figure 2.5. Attenuation of balun.

To design our transmission lines, we show in Figure 2.6 the relationship between the conductor size and spacing for the two twinline configurations shown in Figure 2.1. For round wires the relationship is given in Equation (1) and for the coplanar strips the relationship is given in [2]. For the plots in Figure 2.6, the desired impedance of the line is 200 Ω. For the coplanar strips the dielectric is 0.35 mm (0.014″) thick, with a relative dielectric constant of 2.5 (combination of Kapton®, polyester, and adhesive). The conductive strips are assumed to be infinitely thin. This theory provides a useful starting point, but the theoretical dimensions must be refined through experiment.

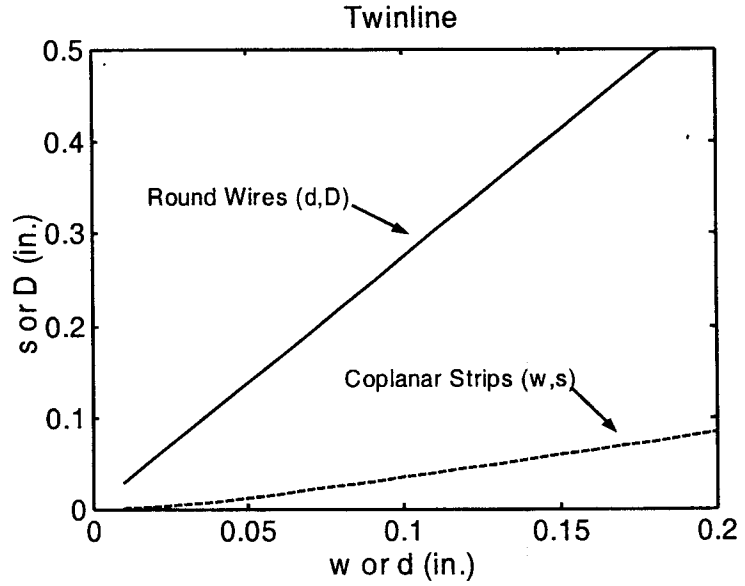

Figure 2.6. Relationship between the conductors in two twinline configurations.

III. Membrane Materials and the Etching Process.

The Phase I Membrane IRA was fabricated from commercially available flat films. We designed the pattern for the gore segments of the reflector so that the singly curved segments would be a good approximation of the doubly curved paraboloid. The gore segment for the Collapsible Impulse Radiating Antenna (CIRA) was modified to allow for pressure acting on the entire reflector surface.

Since the reflector and feed arms of the Membrane IRA require a conductive surface, we constructed the antenna from aluminized Kapton®, with aluminum 300 angstroms thick. The use of aluminized Kapton® required that some of the aluminum be stripped from the Kapton® to create the desired conductor shapes. We ran a series of tests using various solvents to remove the aluminum from the Kapton® and found that acetone produced the best results. The results of masking an area and stripping the aluminum with acetone can be seen in Figures 3.1-3.3. There was some concern about the smoothness of the stripped edges, so we examined these under a microscope. Figures 3.2 and 3.3 show that the stripping procedure does not leave a microscopically smooth edge. The remaining "jaggies" in our test were on the order of 0.1 mm in size. We believe that this is sufficiently accurate for our purposes. Alternatively, we could also consider printing the metallization onto the membrane. This method may be preferable for both the large conductive surfaces and for the twinline used for the antenna feed.

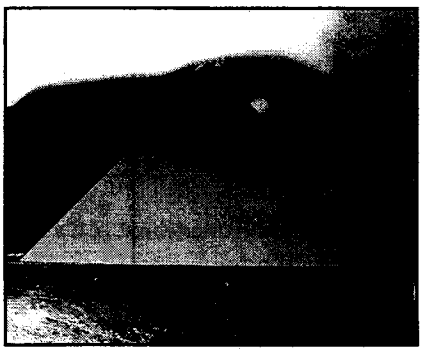

Figure 3.1.
Stripped triangle.

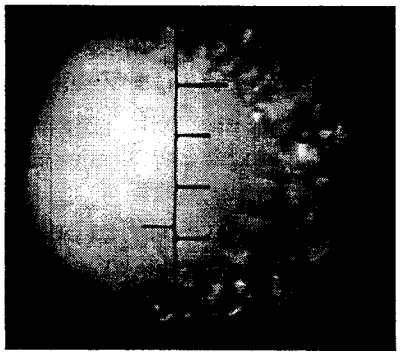

Figure 3.2.
Close-up of triangle corner.

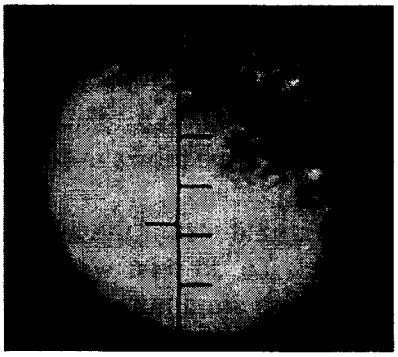

Figure 3.1.
Close-up of triangle edge.

(Note that each increment shown on the microscopic scale is 0.1mm)

IV. Reflector Conductor Thickness.

Next, we evaluate the plating thickness needed for the aluminum-coated Kapton® to perform as an RF reflector. First, we consider the skin depth of the aluminum on the Kapton® film. The skin depth of a conductor is given by

$$\delta = \frac{1}{\sqrt{\pi \sigma \mu_o f}} \tag{6}$$

where $\sigma = 3.57 \times 10^7$ mho/m for aluminum and $\mu_0 = 4\pi \times 10^{-7}$ H/m. At 10GHz the skin depth is 8.5×10^3 angstroms (850 nm). This is approximately 28 times the thickness of the aluminum, and the skin depth increases at lower frequencies. Normally, we would like a conductor to be several skin depths thick at the frequencies of interest. Fortunately, that will not be needed, as we demonstrate below.

A second way of checking our conductor thickness is to calculate the surface impedance in ohms/square of the thin layer of aluminum. If the surface impedance is small compared to 377 Ω, then the material will act as a conductor. We calculated the surface impedance using the formula

$$Z_s = \frac{1}{\sigma t} \tag{7}$$

where t is the thickness of the aluminum coating. This formula gives the impedance one would measure with a dc ohmmeter across opposite sides of a square piece of the coated membrane. Using the above values, we calculate Z_s = 0.93 Ω/square, which should be low enough to act as a good reflector. We measured the surface impedance of the membrane with an ohmmeter, and we found it to be approximately 0.7 Ω/square, which is quite close to the predicted value. While this is several times the resistivity of the fabric used in the CIRA, we believe this is still low enough to be effective.

As a final test of the aluminum thickness, we carried out free-space reflection measurements of the material. To do this, we made TDR measurements of a Farr Research Model TEM-1-50 sensor with both solid aluminum (1.6mm thick) and the aluminized Kapton® (300 Å thick) placed in front of the sensor. The results are shown in Figure 4.1, where we see that there is little difference between the two TDRs. Thus, both materials reflect the field equally well. Note that the horizontal line from about 1 to 9 ns is the 50-ohm impedance of the TEM horn, and that the reflection from the aluminum is the dip in signal at around 9.5 ns on the two plots. If the aluminum is removed, the dip goes away.

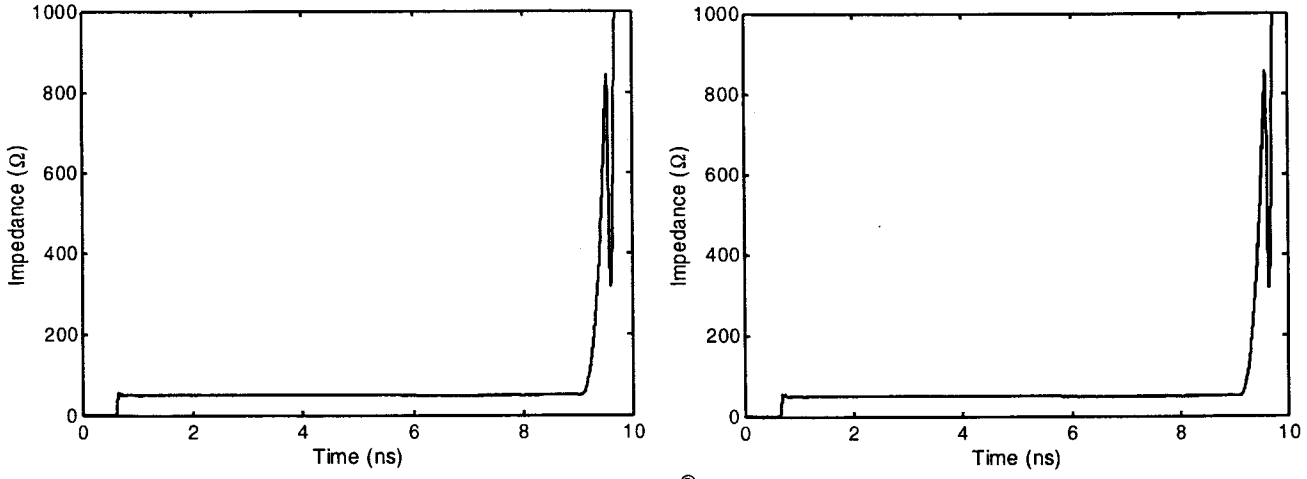

Figure 4.1. Comparison of TDRs with Al on Kapton® (left) and 1.6mm (1/16″) thick Al Plate (right).

V. Fabrication and Measurement of the Membrane IRA.

We designed and constructed a four foot diameter Membrane IRA, fabricated using aluminized Kapton® and Mylar®. The membrane was 1-mil thick Kapton with a 300-angstrom thick aluminum coating. The parabolic reflector was 1.22 m (48″) in diameter with a focus of 0.488 m (19.2″) (F/D = 0.4). The reflector was made of 12 panels of flat membrane material cut and bonded together to closely approximate a true parabola.

The shape of the prototype closely resembles the Collapsible IRA (CIRA) built previously by Farr Research, with the exception of feed arm alignment. Normally, the charge center of the feed arms is aligned with the rim of the reflector. However, this seemed difficult to implement on a Membrane IRA, because of the difficulty in manufacturing "floppy" feed arms that extend beyond the reflector rim. For that reason, we aligned the outer edge of the feed arms with the rim of the reflector. Calculations by J. S. Tyo have shown that this has little effect on the numerically calculated h_a on boresight [3].

An early design of the prototype Membrane IRA is sketched in Figure 5.1. The feed arms are placed at ±30° to vertical. This configuration improves the performance of the IRA as predicted in [3] and experimentally verified in [4]. The parabolic reflector is plated with aluminum, except in a region between the feed arms, where the E field points in the wrong direction. A sketch of this region is shown in Figure 5.2 [5].

The as-built assembly drawing of the Membrane IRA is shown in Figure 5.3. Here, we see that the support torus in Figure 5.1 has been removed, and a conical support structure has been added. Figure 5.4 is a photograph of the Membrane IRA in a collapsed configuration for shipping. In Figure 5.5 we show the conical support structure prior to attaching the Membrane IRA. The inflated Membrane IRA is shown in Figure 5.6 during testing at the outdoor antenna range. The inflation tube is shown on the right in the picture. The inflation pressure was approximately 12.5 Pa (0.05 inches of water).

For the prototype Membrane IRA we had planned to use round wires for the twinline feed as described above. However, during construction of the antenna, it was decided that coplanar strips would be simpler to build. The twinline coplanar strips were constructed of self-adhesive copper tape that were 1.6 mm (0.065″) wide by 0.086 mm (0.0034″) thick. The distance between the strips was 0.51 mm (0.020″).

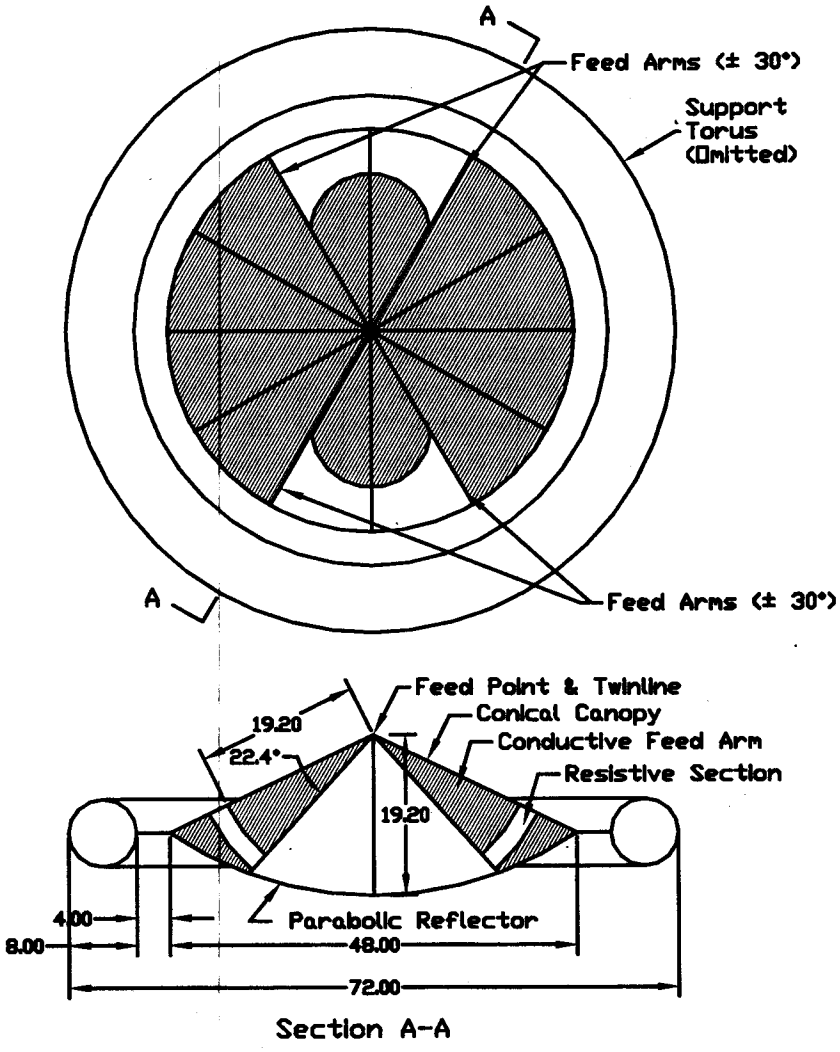

Figure 5.1. Design of the Membrane IRA.

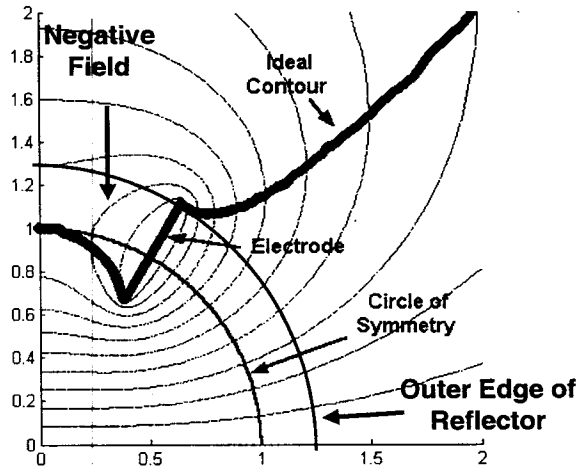

Figure 5.2. Sketch of the aperture fields of one-quarter of an IRA reflector. Note the Region of Negative Field Contribution, where conductor in the reflector should be removed.

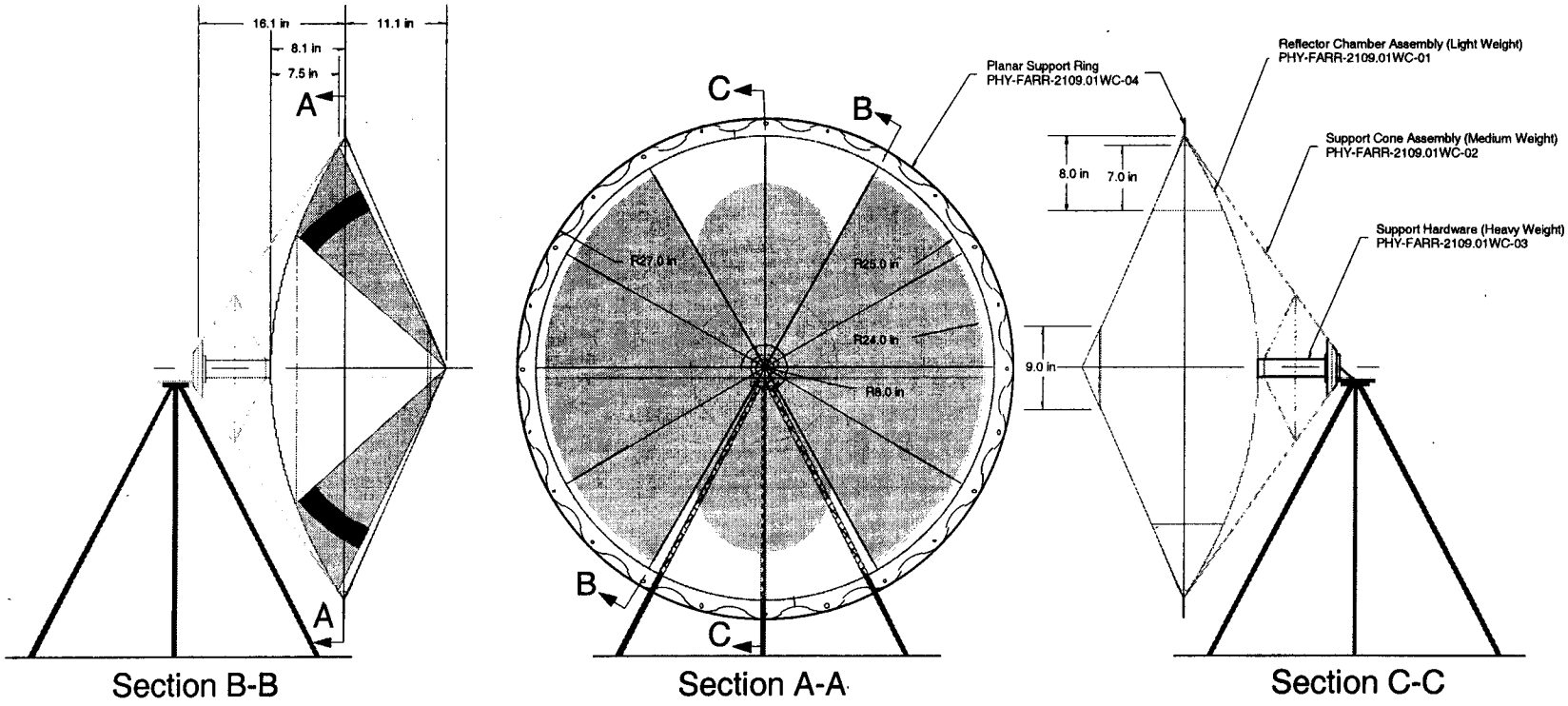

Figure 5.3. Assembly drawing of the Membrane IRA.

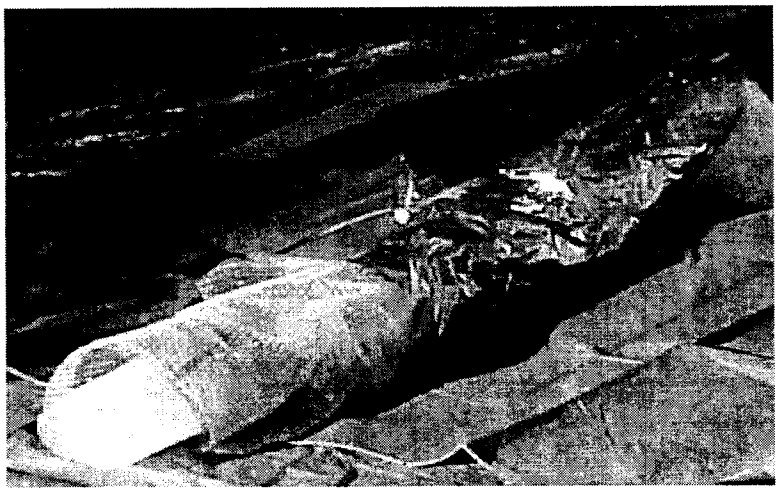

Figure 5.4. Rolled Membrane IRA.

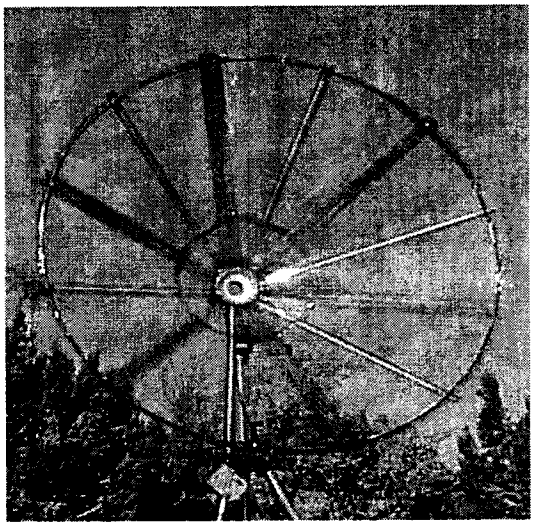

Figure 5.5. Support cone.

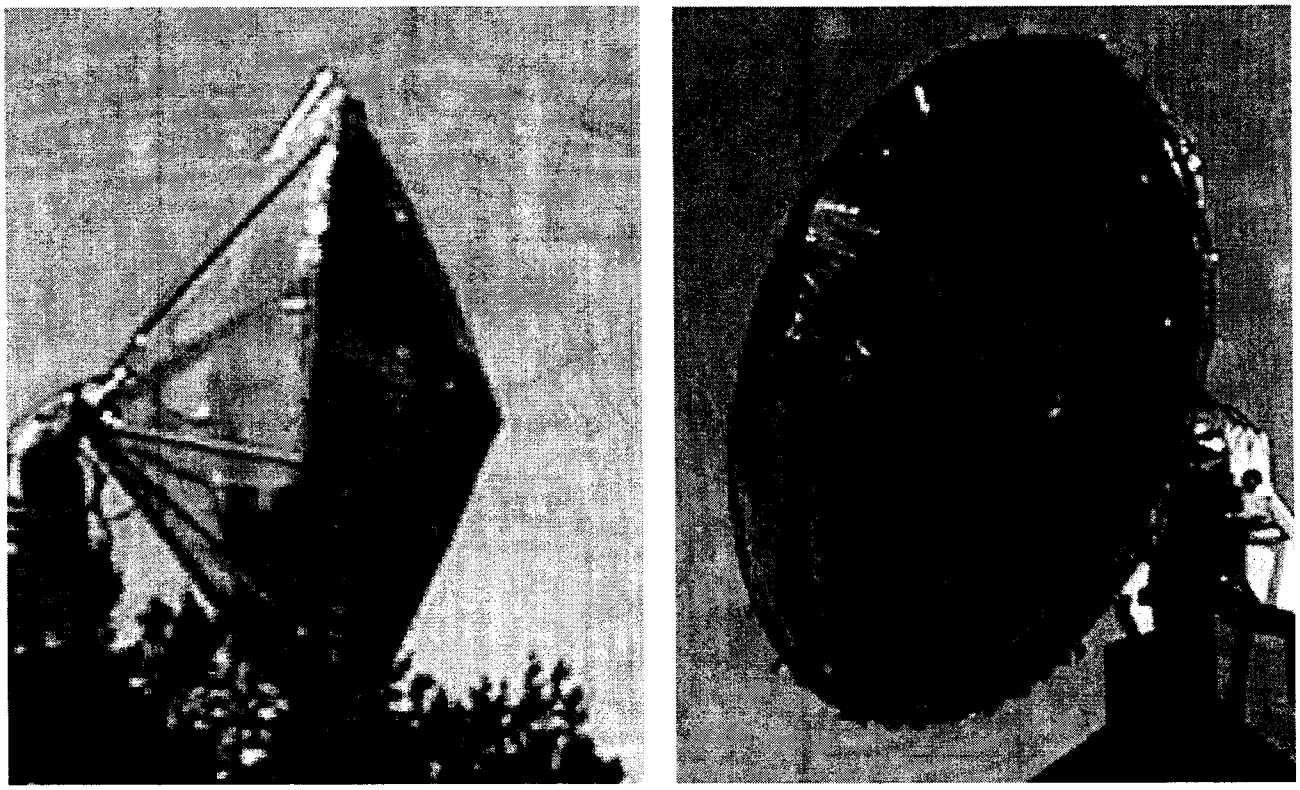

Figure 5.6. Inflated Membrane IRA during RF characterization.

We began our characterization of the prototype with a measurement of the TDR, as shown in Figure 5.7. Ideally, we should observe a flat 50 ohms throughout the entire structure, but the actual device deviates from this somewhat. We are using a custom splitter built by Farr Research, so the splitter is almost invisible in the TDR. Thus, the impedance is very close to 50 ohms up to the junction

with the twinline. The twinline is surprisingly smooth, considering that it was handmade, but it has an apparent impedance of 4 × 35 ohms = 140 ohms, instead of the 200 ohms for which it was designed. (The factor of four multiplier is caused by the balun.) It is simple to adjust the twinline impedance by separating the lines a little more. Along the length of the feed arms, however, we have a more serious problem. The apparent impedance jumps to 4 × 170 ohms = 680 ohms, where it should be just 200 ohms. We suspect that this is due to a poor contact make at the reflector focus between the twinline and feed arms. The contact was made only with copper tape, but in the future it will have to be bonded in a better way. A post-test experiment showed that the TDR could be improved greatly by soldering the connections at the feed point. We also suspect a poor electrical contact at the junction between the ends of the feed arms and the load resistors, since only conductive adhesive was used to make the connection.

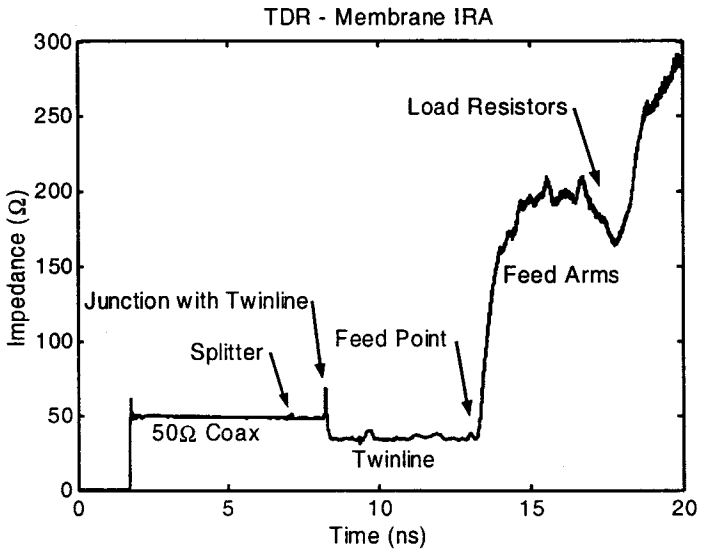

Figure 5.7. TDR of Membrane IRA

Next, we made antenna pattern measurements at our time domain antenna range. The measurements were made at a distance of 20 m, using a Picosecond Pulse Lab Model 4015C source, with risetime of 20 ps and peak output of 4 V. The oscilloscope was the Tektronix TDS 8000, with risetime of 17 ps. The sensor was a Farr Research Model FRI-TEM-01-50 TEM horn sensor, with FWHM = 31 ps. In Figure 5.8 we show the normalized impulse response. This antenna has a useful range from 100MHz to 3 GHz as seen in Figure 5.9. The bandwidth can be improved considerably by refining the shape of the reflector and feed arms and by improving the construction of the feed point.

The antenna pattern based on the peak value of the normalized impulse response is given in Figure 5.10. It was very difficult to adjust the antenna direction precisely, so the peak occurred slightly off zero degrees in the H plane. This means that all the measurements in the E plane were made slightly to one side of boresight in the H plane. This contributes to the somewhat strange appearance of the pattern in the E plane.

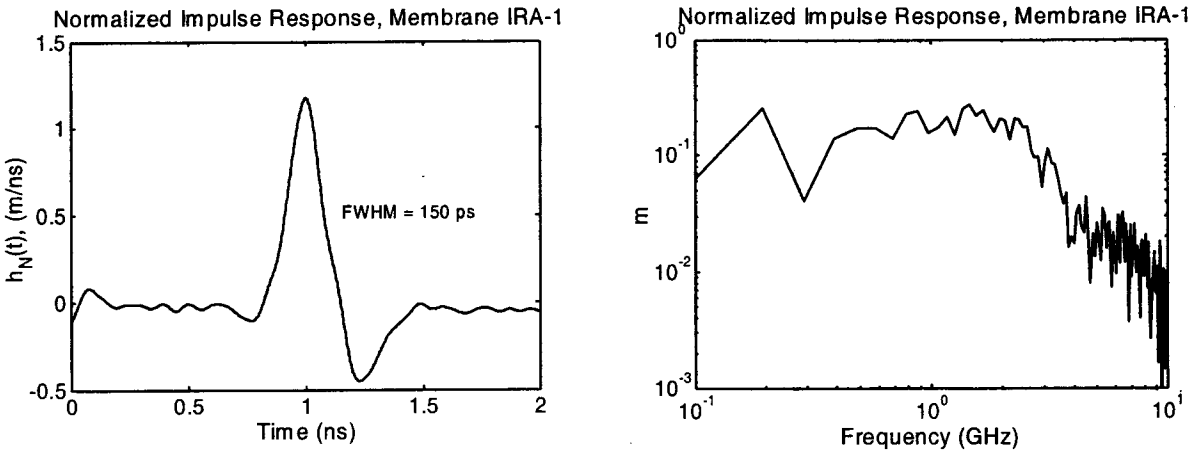

Figure 5.8. Normalized Impulse Response in the time and frequency domains.

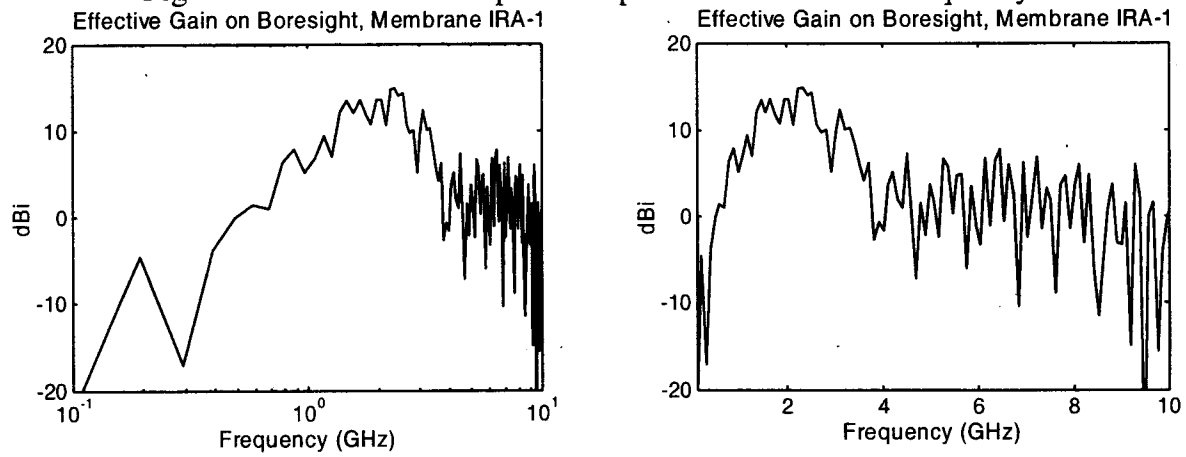

Figure 5.9. Effective Gain of the Membrane IRA.

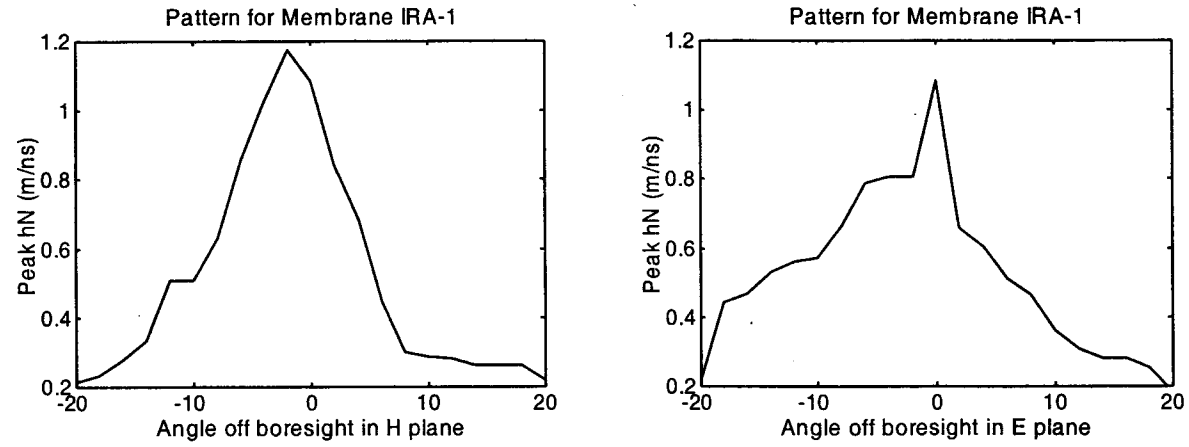

Figure 5.10. Pattern of the Membrane IRA in the H and E planes.

VI. Discussion.

The performance of our first membrane IRA is quite a bit below that of our first CIRA. We suspect that the biggest reason for this is was the poor connection at the feed point near the reflector focus. This could easily be addressed by using a solder connection instead of conducting epoxy to make the bonds. The balun and feed line performed quite well, and this opens up new possibilities for feeding all IRAs.

To take the next step in the membrane IRA, it would be necessary to replace the umbrella-like supporting cone with an inflatable toroidal support. The antenna would also need to be hardened against puncture by small space-borne particles, either by providing makeup gas or by rigidizing the antenna. Finally, it would be necessary to use only materials suitable for the extreme thermal and radiation environment.

Since beginning this project, we have come to believe that, for space antennas of modest size, the preferred IRA design is a variation of the umbrella-like CIRA. The proposed variation would have Z-folded ribs and a telescoping center support, much like compact rain umbrellas. Such a device could be deployed by tripping a latch with a spring-loaded mechanism. This new design will likely become the focus of our future work, because our intended application does not require a large diameter or high gain. We believe that inflatable designs are likely to be more suitable for much larger antennas, where an umbrella is not feasible.

VII. Conclusions.

We have shown that a useful antenna can be built using aluminized Kapton® for the reflector and feed arms and non-metallized Kapton® for the inflatable envelope. For large reflector IRAs this technique would be the construction and deployment method of choice. However, we have learned that for antennas of the size of the one described here, the preferred construction is based on a mechanical deployment/support system similar to the CIRA but much more compact and light weight.

One of the most interesting and worthwhile results of this work is the development of the new feedline/balun configuration. This configuration makes it possible to have a very flexible connection to the feed point using a transmission line plated onto the membrane material, rather than using the standard feed that requires two coax cables. This new balun opens up new possibilities in many IRA designs, and will likely be incorporated into the new more compact CIRA designs that will be explored next.

References.

1. L. H. Bowen, E. G. Farr, and W. D. Prather, "An Improved Collapsible Impulse Radiating Antenna, Sensor and Simulation Note 444, April 2000.

2. B. C. Wadell, *Transmission Line Design Handbook*, Artech House, Boston, 1991.

3. J. S. Tyo, "Optimization of the Feed Impedance for an Arbitrary Cross-Feed-Arm Impulse Radiating Antenna," Sensor and Simulation Note 438, November 1999.

4. L. H. Bowen, E. G. Farr, C. E. Baum, T. C. Tran, and W. D. Prather, "Experimental Results of Optimizing the Location of the Feed Arms in a Collapsible IRA and Solid IRA," Sensor and Simulation Note 450, November 2000.

5. J. S. Tyo, Personal Communication.